

Pretrained Embeddings as a Behavior Specification Mechanism

Parv Kapoor

Carnegie Mellon University

PARVK@ANDREW.CMU.EDU

Abigail Hammer

Carnegie Mellon University

ARHAMMER@ANDREW.CMU.EDU

Ashish Kapoor

Scaled Foundations

ASHISH@SCALEDFOUNDATIONS.AI

Karen Leung

University of Washington

KYMLEUNG@UW.EDU

Eunsuk Kang

Carnegie Mellon University

EUNSUKK@ANDREW.CMU.EDU

Abstract

We propose an approach to formally specifying the behavioral properties of systems that rely on a perception model for interactions with the physical world. The key idea is to introduce *embeddings*—mathematical representations of a real-world concept—as a first-class construct in a specification language, where properties are expressed in terms of distances between a pair of ideal and observed embeddings. To realize this approach, we propose a new type of temporal logic called *Embedding Temporal Logic (ETL)*, and describe how it can be used to express a wider range of properties about AI-enabled systems than previously possible. We demonstrate the applicability of ETL through a preliminary evaluation involving planning tasks in robots that are driven by foundation models; the results are promising, showing that embedding-based specifications can be used to steer a system towards desirable behaviors.

1. Introduction

Modern artificial intelligence (AI) technologies, such as foundation models (FMs), are rapidly merging as a key component in autonomous systems, being used to perform critical functions such as perception and planning. Techniques for achieving high assurance, such as verification and runtime monitoring, rely on the availability of *formal specifications* that capture the desired properties of a system. However, formally specifying the behavior of an AI-enabled system remains an open challenge [Seshia et al. \(2018\)](#).

Formal specifications, especially those written in a temporal logic, are expressed in terms of propositions about parts of the system state that can be observed or estimated through sensors (e.g., the velocity of a robot).

For autonomous systems, behavioral properties often refer to interactions with physical objects (e.g., “the robot should avoid colliding with a table”); to observe these objects, the system relies on a perception model that operates over a high-dimensional input image. A formal specification for such a system would require propositions that relate physical objects to the input image. Here lies the fundamental obstacle to specification: devising a precise, mathematical encoding of a physical object (e.g., a table) over the high-dimensional input space (e.g., pixels) is likely to be difficult, if not impossible.

In this paper, we propose a new approach for formally specifying the behavioral properties of an AI-based system. The key idea is to introduce *embeddings*—mathematical representations of real-world objects—as a first-class concept in a specification notation, and express a property in terms of *distances* between a *target* embedding (an ideal representation of the world for the system to reach or avoid, given as part of the specification) and an *observed* embedding (a representation observed and generated through a sensor during system execution). For example, consider a rescue robot that is tasked with satisfying the following requirement: “Locate a potential victim while avoiding areas with fire.” Such a property would be difficult to specify using an existing specification language, due to its dependence on perception; even with access to accurate localization, the exact locations of these real-world objects are often unknown and dynamic. Instead, in an embedding-based approach, this task may be expressed as “reach the state of the world in which the system observes an object that closely resembles a potential victim, while avoiding those states where the observation resembles an area with fire.” Such a specification could then be used, for example, as part of a run-time monitor or a planner to ensure that the system conforms to the desired property.

As a realization of this approach, we propose *Embedding Temporal Logic (ETL)*, a temporal logic for specifying the behaviors of AI-based systems (Section 3). Compared to state-based temporal specifications (such as linear temporal logic (LTL) [Pnueli \(1977\)](#)), which are evaluated over a sequence of states, an ETL specification is evaluated over a *sequence of embeddings*, where each embedding is created from an observation that the system makes at a particular point in its execution. As counterparts to propositions in LTL, atomic constructs in ETL are *embedding predicates*, which impose a constraint over the distance between a pair of embeddings; e.g., $\text{dist}(z_o, z_t) \leq \epsilon$, where z_t and z_o are the target and observed embeddings, respectively, and $\epsilon \in \mathbb{M}$ is a given *distance threshold* in metric space \mathbb{M} . A target embedding in a predicate is specified by providing images or text that correspond to a real-world concept (e.g., images or a textual description of fire). Standard temporal operators (e.g., **G**, **F**) are used to construct temporal properties out of atomic predicates.

We believe that **embeddings as a specification mechanism** have potential to **significantly broaden the range of properties that can be specified using a formal specification language**, facilitate the development of new assurance methods, and enable existing methods to be applied to AI-enabled systems. Additionally, leveraging embeddings for specification allows us to use the power of large, pretrained FMs [Radford et al. \(2021a\)](#); [Firoozi et al. \(2023\)](#)—which excel at encoding high-level features and concepts into embedding spaces. Moreover, integrating world models [Ha and Schmidhuber \(2018\)](#) that evolve within these embedding spaces further enriches our ability to reason about and verify the dynamic behaviors of such systems. As a potential application, we demonstrate how ETL can be used for *planning* tasks in robotic systems that use an FM for scene understanding and behavioral prediction (Section 4). In particular, we propose a planning method that generates actions towards the goal of satisfying a given ETL specification. Our preliminary evaluation shows that the proposed method can effectively steer the system towards behaviors that are desirable with respect to the given specification (Section 5).

2. Background

We briefly describe the ideas of pretrained vision models and world models, which play an important role for embeddings and FM-based planning, respectively.

Pretrained Vision Models. Pretrained vision models such as CLIP [Radford et al. \(2021b\)](#), DINOv2 [Oquab et al. \(2024\)](#) have revolutionized the field of computer vision by providing robust, high-

level representations that capture rich semantic information. These models are generally trained on large-scale datasets and use supervised or self-supervised learning methods. The resulting representations (embeddings or feature vectors) have demonstrated impressive transferability across a wide range of downstream tasks including classification, detection, segmentation, and scene understanding. These models are built with convolutional neural networks (CNNs) [Krizhevsky et al. \(2012\)](#) or more recently vision transformers (ViTs) [Dosovitskiy et al. \(2021\)](#). ViT based models generally take as input a raw image and generate patch embeddings capturing granular information.

World Models. In the context of *sequential decision-making* for robots—the process of generating a sequence of actions to enable a system to perform a desired task—a robot must be able to predict future outcomes given their decisions. Such predictive models are generally referred to as *world models* [Ha and Schmidhuber \(2018\)](#), describing *how the world evolves over time*. Abstractly, the “world” includes the robot itself, the surrounding environment, and interactions between the two. However, in unstructured settings without accurate state estimation and scene understanding, developing a world model operating on observations (e.g., camera images) can be challenging.

Many recent works look to develop a world model by leveraging large amounts of offline observation data (e.g., images) collected from the system moving in the real-world and learning the transition dynamics of the system implicitly through a lower-dimensional embedding space [Ha and Schmidhuber \(2018\)](#); [Watter et al. \(2015\)](#). We follow a similar set up as described in [Zhou et al. \(2025\)](#). The idea is to encode the high-dimensional observations during a time window H , (starting from time $t - H$ to t , denoted $o_{t-H:t}$), into corresponding embedded states $z_{t-H:t}$. The embedded states and control sequence $a_{t-H:t}$ are inputs to a learned transition model p to predict the latent state in the next time step z_{t+1} . A decoder q can transform embedded states back into observation states \hat{o} —the decoder is not strictly needed in describing how the world evolves, but rather is more useful for visualizing what observation the latent state corresponds to. Mathematically, a world model consists of the following three components,

$$\underbrace{z_t \sim \text{enc}_\theta(z_t \mid o_t)}_{\text{Observation model}}, \quad \underbrace{z_{t+1} \sim p_\theta(z_{t+1} \mid z_{t-H:t}, a_{t-H:t})}_{\text{Transition model}}, \quad \underbrace{\hat{o}_t \sim q_\theta(o_t \mid z_t)}_{\text{Decoder model}}, \quad (1)$$

where θ denotes the parameters of the encoder (enc), decoder, and transition models. Essentially, at any time step t , we can compute the latent state z_t , and autoregressively roll out the transition model to simulate how the world evolves given a sequence of actions.

3. Embedding Temporal Logic

3.1. Syntax and Semantics

In our approach, a system is assumed to make an observation about the real world through a sensor (e.g., camera) at each step in its execution. The system also contains an *encoder* that converts each observation into an embedding $z \in \mathcal{Z}$. Conceptually, z is an approximation of a *latent variable*; i.e., the state of the world that is only indirectly observable by the system. The underlying representation of embeddings (typically as a vector of a fixed size) depends on the encoder and other models that subsequently consume this embedding for further tasks, such as object identification and prediction.

In ETL, a possible execution of the system, or a *trace*, is represented as an infinite sequence σ of embeddings (i.e., $\sigma = z_0, z_1, \dots$); we write z_i to denote the embedding at the index i . We also assume the existence of *distance function* $\text{dist} : \mathcal{Z} \times \mathcal{Z} \rightarrow \mathbb{M}$, which computes a distance between

a pair of embeddings. The metric space depends on the embedding representation and the distance function used; a common option is $\mathbb{R}^{\geq 0}$. The syntax of ETL is as follows:

$$\varphi := u \mid \neg\varphi \mid \varphi_1 \wedge \varphi_2 \mid \varphi_1 \mathbf{U} \varphi_2$$

where u is a predicate of the form $f_u(z) > 0$ and $f_u(z)$ is the function (associated with u) that maps the current embedding z to a value in the metrics domain \mathbb{M} . As in LTL, the until operator \mathbf{U} can be used to express the *eventually* (\mathbf{F}) and *always* (\mathbf{G}): $\mathbf{F}\varphi = \text{True} \mathbf{U} \varphi$ and $\mathbf{G}\varphi = \neg \mathbf{F} \neg \varphi$.

The semantics of ETL, defining the satisfaction of a formula by trace σ at index i , also closely mirrors that of LTL:

$$\begin{aligned} \sigma, i &\models u \iff f_u(z_i) > 0 \\ \sigma, i &\models \neg\varphi \iff \sigma, i \not\models \varphi \\ \sigma, i &\models \varphi_1 \wedge \varphi_2 \iff \sigma, i \models \varphi_1 \text{ and } \sigma, i \models \varphi_2 \\ \sigma, i &\models \varphi_1 \mathbf{U} \varphi_2 \iff \exists j \geq i \text{ such that } \sigma, j \models \varphi_2 \text{ and } \forall k \text{ with } i \leq k < j, \sigma, k \models \varphi_1 \end{aligned}$$

Example 1: Reach and Avoid. A common task in robotic systems involves reaching a particular goal (i.e., a location); e.g., “a system shall eventually navigate to the desired location” while avoiding unsafe regions. The unsafe region requirement can be described at a high level as “the system should avoid hazardous areas.” Given an embedding $z_g \in \mathcal{Z}$ representing the goal location and a finite set of embeddings $Z_{\text{avoid}} = \{z_{a_1}, \dots, z_{a_m}\} \subseteq \mathcal{Z}$ (where $m = |Z_{\text{avoid}}|$), representing the hazardous areas, this requirement can be specified in ETL as: $\mathbf{F}(\text{dist}(z, z_g) \leq \epsilon_g) \wedge_{i=1}^m \mathbf{G}((\text{dist}(z, z_{a_i}) > \epsilon_{a_i})$ where the robot’s location embedding is z , ϵ_g the minimum closeness required for reaching the goal, and $(\epsilon_{a_1}, \dots, \epsilon_{a_m})$ the minimum safe distances that must be maintained from the hazardous areas.

Example 2: Sequential task. Another common type of tasks for robotic systems is to visit multiple goals in a sequence. This pattern is sometimes called *sequenced visit* Menghi et al. (2019). Given two embeddings $z_{g_1}, z_{g_2} \in \mathcal{Z}$ that represents the two goal locations, the requirement can be specified as an ETL specification that requires the distance from the robot and the locations to fall below a given threshold ϵ_g , one after another: $\mathbf{F}((\text{dist}(z, z_{g_1}) \leq \epsilon_{g_1}) \wedge \mathbf{F}(\text{dist}(z, z_{g_2}) \leq \epsilon_{g_2}))$.

Example 3: Stability. In *visual servoing* Hutchinson et al. (1996), a robot adjusts its movements to align its camera view with a target reference image, using visual feedback rather than explicit position measurements. A key requirement in such systems is *stability*, ensuring that once the desired visual state is reached, the system constantly remains in the same region of the embedding space; e.g., “once a drone reaches a desired viewpoint, it should maintain the viewpoint.” Given an embedding $z_g \in \mathcal{Z}$ representing the target visual state, stability can be specified in ETL as: $\mathbf{FG}(\text{dist}(z, z_g) \leq \epsilon_g)$ where: ϵ_g ensures that once the system achieves the desired visual embedding, it maintains that state indefinitely.

3.2. Quantitative Satisfaction

Certain extensions of LTL, such as *signal temporal logic* (STL) Maler and Nickovic (2004), allow for a quantitative notion of satisfaction (called *robustness* Fainekos and Pappas (2009)) that represents the degree to which the system satisfies or violates a specification. Among its use cases, robustness can be leveraged in *optimization-based tasks*, such as trajectory planning Raman et al.

(2014), where the quality of candidate plans is evaluated based on how well the resulting system behavior satisfies a property (i.e., the robustness score). To enable ETL to be used for such tasks (later discussed in Section 4), we also introduce a notion of quantitative satisfaction for ETL.

The *satisfaction score* of a trace with respect to ETL formula φ at index i , bounded by $\mathbf{b} \geq i$, is denoted $\rho(\varphi, \sigma, i, \mathbf{b})$ and defined as follows:

$$\begin{aligned}\rho(u, \sigma, i, \mathbf{b}) &= f_u(z_i) \\ \rho(\neg\varphi, \sigma, i, \mathbf{b}) &= -\rho(\varphi, \sigma, i, \mathbf{b}) \\ \rho(\varphi_1 \wedge \varphi_2, \sigma, i, \mathbf{b}) &= \min(\rho(\varphi_1, \sigma, i, \mathbf{b}), \rho(\varphi_2, \sigma, i, \mathbf{b})) \\ \rho(\mathbf{G}\varphi, \sigma, i, \mathbf{b}) &= \inf_{k \in [i, \mathbf{b}]} \rho(\varphi, \sigma, k, \mathbf{b}) \\ \rho(\mathbf{F}\varphi, \sigma, i, \mathbf{b}) &= \sup_{k \in [i, \mathbf{b}]} \rho(\varphi, \sigma, k, \mathbf{b})\end{aligned}$$

where **inf** and **sup** are the infimum and supremum operators, respectively. Note that the computation of the satisfaction score is restricted to a subsequence of σ between i to \mathbf{b} (i.e., $z_i, z_{i+1}, \dots, z_{\mathbf{b}}$). The bound \mathbf{b} may be determined by, for example, the planning horizon used by a planner (i.e., the length of action sequence used by the planner for behavioral prediction). For brevity, the definition for the until (U) operator is omitted, but similar to the one described in Fainekos and Pappas (2009).

Example. Consider an ETL specification that describes the task of reaching a desired visual state, $\varphi \equiv \mathbf{F}(\text{dist}(z, z_g) \leq \epsilon_g)$, which is equivalent to $\mathbf{F}(\epsilon_g - \text{dist}(z, z_g) > 0)$; i.e., $f_u(z_i) = \epsilon_g - \text{dist}(z_i, z_g)$. Suppose that the system generates a sequence of embeddings of length 4 ($\sigma = z_0, z_1, z_2, z_3$), resulting in the following vector for f_u :

$$[-0.0461393, -0.05276561, 0.08344626, 0.0541718]$$

The satisfaction score of the trace, $\rho(\varphi, \sigma, 0, 4)$, is the maximum value of f_u between the index 0 and 4; i.e., 0.08344626. Intuitively, the satisfaction score of σ corresponds to the point at which the system satisfies the specification most well (i.e., it comes closest to the goal embedding).

3.3. Specifying Target Embeddings

As mentioned above, ETL is specified using predicates over *target embeddings* that describe parts of the physical world to be reached or avoided. In practice, the specifier (e.g., a system engineer) would not directly specify the mathematical representations of embeddings. Instead, a tool that uses ETL (like the planner that we introduce in Section 4) would provide an interface through which the specifier can describe an intended ETL specification with images and/or textual descriptions for the target embeddings. The tool would then use an encoder to translate the user input into the corresponding embeddings, creating the final ETL specification.

We envision that different types of interfaces and patterns can be developed to allow the specifier to build complex ETL specifications, possibly by building on prior works in computer vision and machine learning (ML) for visual and multi-modal task descriptions. For example, in robotics, it has been shown that categorical targets, sets of RGB images (with and without depth), and natural language descriptions can be effectively used as task descriptions Chang et al. (2023).

3.4. Distance Functions

Distance Function between Image Embeddings. Another decision to be made by the specifier is the choice of the distance function between a pair of embeddings. We have investigated four

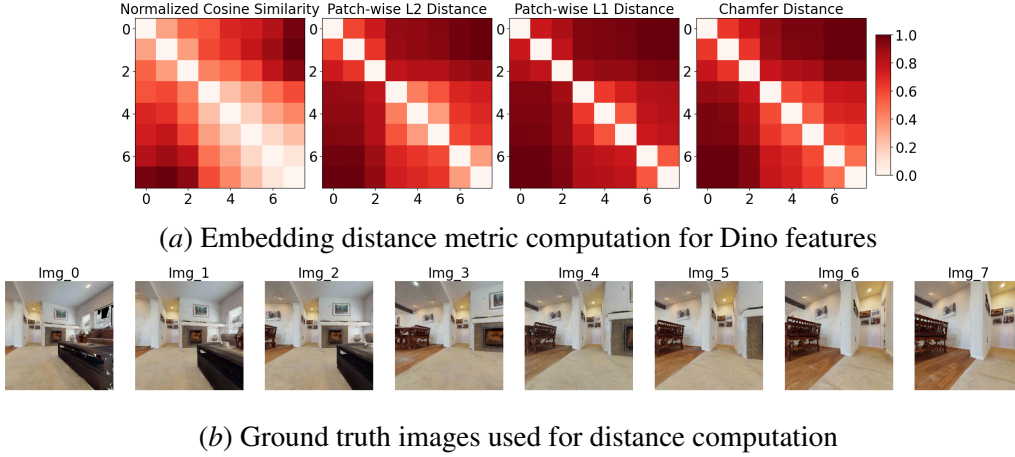


Figure 1: Image-to-image embedding distances We compute distance metrics between the embeddings of images captured within a Habitat scene. Each image is processed by a pretrained encoder, from which we extract the corresponding embeddings. We then calculate the pairwise distances between these embeddings using different distance metrics.

existing distance metrics used in computer vision as candidates for ETL: Cosine similarity, L1, L2, and chamfer distances. Detailed descriptions of these metrics can be found in Appendix A.

We provide an analysis of the suitability of the metrics for capturing distinct visual states. Figure 1(a) shows the distance heatmaps for the four metrics. For each heatmap, we compute pairwise distances between the embeddings of 8 images captured within a Habitat scene Savva et al. (2019) that are generated by a pretrained encoder (DinoV2), as shown in Figure 1(b).

As expected, the diagonal for all embeddings shows zero distance while off-diagonal regions form distinct block-like structures. Frames 0-2 (focused on the fireplace and seating area) cluster together while Frames 6-7 (focused on the dining area) form another cluster. Images within each cluster remain lighter in the heatmap, whereas comparing across the two clusters yields darker blocks.¹

Additionally, the four metrics differ on their emphasis on inter-frame distances. Cosine similarity focuses on embedding orientation, while L2, L1 and chamfer distances measure patch-wise embedding differences. Overall, these heatmaps illustrate how even small viewpoint shifts (e.g. frames 2 vs. 3) can be captured by an increase in embedding distance and can be used to effectively guide behavior generation. Note that distances over raw patch embeddings measure perceptual similarity but lack temporal context as the pretrained vision models are trained on static images. World models transform these embeddings into a learned latent space that evolves based on past states and actions. These world models are trained with a reconstruction loss and hence preserve the structure of the embedding space, ensuring that temporal relationships between embeddings transfer to the latent space. Thus, when using ETL with a world model, it is crucial to select a distance metric that aligns with the training objective of the model.

Image and Textual Embeddings. In addition to images, target embeddings can also be specified using textual descriptions. For brevity, we refer the reader to Appendix B for a discussion of text-to-image embedding comparisons and their role in ETL.

1. A longer version of this figure with more images is available in Appendix A.

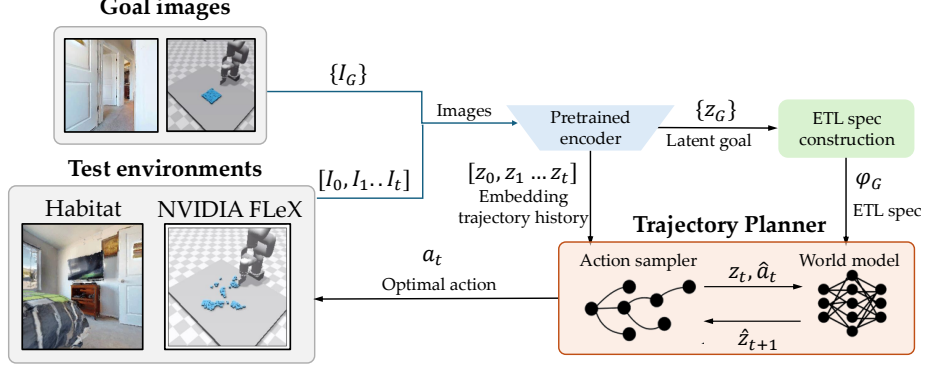


Figure 2: Overview of Planning with ETL specifications We utilize Habitat for navigation and NVIDIA FLeX for granular manipulation. Pretrained encoders generate embeddings from goal and current observations, which are used to evaluate specification satisfaction. The planner integrates these embeddings with a world model to generate ETL satisfying actions.

4. ETL-based Planning

In this section, we propose a method for online robotic planning that generates actions toward satisfying a given ETL specification. The high-level overview of the planning method is highlighted in Figure 2. A key idea is for the planner to leverage a pretrained *world model* when simulating and evaluating candidate actions, and then replan at each time step to perform receding horizon control. Our current prototype accepts image-based ETL specifications but a similar method can be applied for textual specifications as well.

First, our system accepts a set of *goal images*, $\{I_G\}$, from the user and passes them through the pre-trained encoders (e.g., DinoV2 [Oquab et al. \(2024\)](#)/ViT [Dosovitskiy et al. \(2021\)](#)) to generate patch features. Concretely, an input image is divided into fixed-size patches (e.g. 16×16 pixels) that are transformed into a feature vector. These patch features capture localized visual information and are then aggregated by the encoder model to form a global image representation that will serve as reach (z_g) and avoid (Z_{avoid}) embeddings. These embeddings are used to define an ETL specification φ_g (for examples, see Table 1). During the online planning stage, we take the past and current system observations, $[I_0, \dots, I_t]$, and pass them through the same pretrained encoders to compute a corresponding sequence of embeddings, $[z_0, \dots, z_t]$.

Next, the planner generates a set of candidate action sequences, $\hat{a}_t, \dots, \hat{a}_{t+K}$ (where K is the prediction horizon). Each action sequence is executed through the world model to generate a predictive trace (σ). Each predictive trace is then evaluated to compute the satisfaction score for the given specification φ_g , and the action sequence that results in the predictive trace with the highest is selected for the final plan. More formally, this planning process can be expressed as the following optimization problem:

$$a_{t:t+K} = \arg \min_{\hat{a}_{t:t+K} \in \mathcal{A}_{t:t+K}} J_\varphi(z_{0:t+K}) \quad \text{where } \hat{z}_{k+1} = p_\theta(\hat{z}_k, \hat{a}_k), \quad k = t, \dots, K-1, \quad (2)$$

where J_φ is a cost function based on the desired ETL specification. For example, $J_\varphi(z_{0:t+K}) = \max(0, -\rho(\varphi, z_{0:t+K}))$. This cost function penalizes only negative satisfaction scores, i.e., traces that violate φ and ensures that traces satisfying φ (where $\rho(\varphi, z_{0:t+K}) > 0$) have zero cost.

Environment	NL Description	ETL Specification
Navigation	Visit room	$\varphi_1 = \mathbf{F}(\text{dist}(z, z_{g_1}) - \epsilon_{g_1} < 0)$
Navigation	Visit either room	$\varphi_2 = \varphi_1 \vee \mathbf{F}(\text{dist}(z, z_{g_2}) - \epsilon_{g_2} < 0)$
Navigation	Visit rooms sequentially	$\varphi_3 = \mathbf{F}((\text{dist}(z, z_{g_2}) - \epsilon_{g_2} < 0) \wedge \varphi_1)$
Manipulation	Reach configuration	$\psi_1 = \mathbf{F}(\text{dist}(z, z_g) - \epsilon_g < 0)$
Manipulation	Avoid 8 configurations	$\psi_2 = \bigwedge_{i=1}^8 \mathbf{G}(\text{dist}(z, z_{a_i}) + \epsilon_{a_i} > 0)$
Manipulation	Reach and avoid	$\psi_3 = \psi_1 \wedge \psi_2$

Table 1: ETL specifications for navigation and manipulation tasks.

In practice, the number of candidate action sequences is too large to enumerate, so our planner randomly samples N action sequences² and then select the most satisfactory one—an easily parallelizable operation. With the chosen action sequence, the planner applies the first action a_t on the robot, and then repeats the planning process with an updated state (i.e., new sensor image). Note that the world model used here shares the same embedding space as the embeddings used in ETL; operating with a learned world model enables the direct evaluation of ETL quantitative semantics in the embedding space rather than expensively decoding back to the physical state space.

5. Preliminary Evaluation

We describe a preliminary evaluation to demonstrate the potential utility of ETL. In particular, we present experiments involving two types of planning tasks: (1) indoor navigation and (2) robot arm manipulation, to (1) evaluate whether embedding-based specifications can be used to generate plans that result in desirable system behaviors and (2) analyze the impact of different distance metrics.

5.1. Experimental Setup

For indoor navigation, we pre-train a world model on 10,000 expert traces for the PointNav task in the Habitat Environment [Savva et al. \(2019\)](#); Habitat is a photorealistic simulator that creates indoor scenes using real-world assests. We utilize MP3D [Chang et al. \(2017\)](#) assets and build on the Perception Action Causal Transformer (PACT) from a ResNet to a ViT for it’s improved preresentational capacity of ViT [Dosovitskiy et al. \(2021\)](#). We focus on a sampling based planner with multiple cost functions, and plan using sequential specifications, highlighted in Table 1.

For manipulation, we pre-train a DinoWM world model on 2,000 traces leveraging the setup proposed in [Zhou et al. \(2025\)](#) where granules on a flat plane are manipulated into a target goal. To plan the actions, we utilize the integrated Dino World Model planner and measure success by calculating chamfer distances between the final observed image and ground truth goal image, similar to the DinoWM work. We examine three cases of specifications, formalized in Table 1. We baseline against ψ_1 , with a single target specification to reach; for ψ_2 , we provide a set of targets to avoid, and in ψ_3 , we conjunct the requirements of ψ_1 and ψ_2 .

5.2. Results and Discussion

Navigation. , φ_2 , and φ_3) when used with different base distance metrics. As highlighted in Table 2, for φ_1 , the planner is able to achieve positive satisfaction scores with all distance metrics since it

2. Future work can include learning a sampling distribution to increase the quality of action sequence samples.

Distance Metric	Navigation Specifications			Manipulation Specifications		
	φ_1	φ_2	φ_3	ψ_1	ψ_2	ψ_3
L1	0.0031	0.0005	-0.0336	1.04	0.93	0.82
L2	0.0008	0.0035	0.0001	0.99	0.99	0.98
Cosine/CD	0.0021	-0.0046	-0.0274	1.32	1.32	1.32

Table 2: Left: Satisfaction scores for PACT evaluations at a prediction horizon of 15 in navigation tasks. The scores are computed using L2 since PACT was trained using L2 loss defined over predicted and ground truth embedding space. Also, L2 loss had the most granular distance separations as highlighted in Section 4. **Right:** Final chamfer distances (CD) for manipulation tasks, computed over ground truth with a horizon length of 10 in DinoWM.

is a simple reach specification. For φ_2 , we specified the target image embeddings of two different rooms disjuncted with each other, encoding the task of visiting either room. We observe that the planner performs well with L2 and L1 metrics and ends up visiting the physically closest room to its initial location. Additionally, we observed that planning with cosine similarity metric for φ_2 achieves a negative satisfaction score (-0.0046), possibly because it only measures high-level directionality between embedding vectors. As highlighted in Section 4, this leads to scenes with slight perspective change being perceived as similar and hence serve as insufficient feedback for the planner.

In order to evaluate our proposed system’s ability to plan for complex tasks, we used a complex sequential visit specification (φ_3) that involved exploring multiple rooms. Due to this task complexity, planning with L1 and cosine similarity distance-based specifications achieve negative satisfaction scores (-0.0036 and -0.0274 , respectively).

For these metrics, we observed that the planner was able to satisfy the first phase of the task but failed to achieve the second phase of visiting the other room. However, with the L2-based distance metric, the planner is able to generate actions that guide it to the second room. We provide qualitative image results in Appendix C.

In summary, the results suggest that ETL can be used to specify desired system behaviors, and its quantitative semantics can be leveraged by a planner to steer the system towards behaviors that satisfy a given specification.

Manipulation. We performed planning for the reach (ψ_1), avoid (ψ_2), and reach-avoid (ψ_3) specifications using distance metrics of the L1 norm, L2 norm, and chamfer distances (CD) of the embedded images.

In Table 2, we present the ground truth chamfer distances computed after planning with a horizon of length 10. We can observe that for L2 and CD, the ending distances are very similar; however, we can also note that the results for specification ψ_2 shows a reduction in the final chamfer distance. Even without a goal to plan towards, DinoWM is able to infer from the avoid embeddings that the granules should not be in a scattered configuration, and arranges them into a grouping. From this, we hypothesize that the reach-avoid specification ψ_3 shows strong similarity to the reach specification ψ_1 due to optimization done during planning. From these results, we can conclude ETL specifications used during planning are able to successfully perform manipulation tasks. An additional discussion of the results is provided in Appendix D.

6. Related Work

There is a long line of work on specifying and verifying complex behaviors in cyber-physical and robotic systems using temporal logics, such as LTL, STL, and Metric Temporal Logic (MTL) [Koymans \(1990\)](#). These logics have been used for trajectory planning [Kress-Gazit et al. \(2009\)](#); [Sun et al. \(2022\)](#); [Leung et al. \(2023\)](#), reinforcement learning [Aksaray et al. \(2016\)](#); [Alur et al. \(2023\)](#); [Aloor et al. \(2023\)](#), runtime monitoring [Bartocci et al. \(2018\)](#), and adaptive control [Raman et al. \(2014\)](#); [Belta and Sadraddini \(2019\)](#); [Lindemann and Dimarogonas \(2019\)](#); [Kapoor et al. \(2025\)](#).

The logics outlined above can struggle with systems that rely on ML for perception, where input data can have a variable number of objects in frames and evolving bounding boxes. This has led to spatial extensions of STL and MTL that allow one to specify properties with geometric interpretations [Haghighi et al. \(2015\)](#); [Bortolussi and Nenzi \(2014\)](#). Specialized logics such as Timed Quality Temporal Logic (TQTL) [Dokhanchi et al. \(2018\)](#) and Spatio-Temporal Quality Logic (STQL) [Hekmatnejad \(2021\)](#); [Balakrishnan et al. \(2021\)](#) have been proposed for perception systems that permit reasoning about properties over bounding boxes used in object detection. Recently, Spatiotemporal Perception Logic (STPL) [Hekmatnejad et al. \(2024\)](#) was introduced that combined TQTL with spatial logic and allows quantification over objects, as well as 2D and 3D spatial reasoning. STPL allows expressing properties by specifying relations between objects over time. Most of these logics are grounded in the symbolic outputs of a perception module (object labels, confidences, track IDs). In comparison, ETL is used to specify properties directly about the embedding space, making it easier to specify tasks such as “go to an area like this image” without depending on object detection models or their object vocabulary. Additionally, ETL can potentially be specified using textual descriptions as well (using CLIP text embeddings [Radford et al. \(2021b\)](#)), allowing for multimodality in specification, in line with recent advances in pre-trained models for robotics [Firoozi et al. \(2023\)](#).

7. Open Challenges and Future Work

Based on our preliminary investigation, we believe that ETL—and more generally, embeddings as a specification construct—presents a promising approach to specifying a wide range of properties about AI-enabled systems. Beside the planning use case presented in this paper, we envision that ETL could be applied to other assurance tasks, such as online monitoring, falsification, and verification. Here, we discuss some open challenges and paths forward for making embedding-based specifications more applicable and practical.

The benefit of operating on explicit and fully observable states (e.g., position) is that the distance metrics are spatially grounded. For instance, if the euclidean distance between a position (x, y) and an obstacle is, say 1, then that can be directly interpreted as the physical distance of one meter. However, interpreting distances in the embedding space is less spatially grounded. For instance, what does an embedding distance of 0.1 mean between two images? A low number suggests higher similarity, but *how* are they similar? Defining thresholds for embedding distances is an open challenge for ETL. As one potential direction, we envision that existing ML techniques could be leveraged for threshold definition. For example, we could potentially calibrate or perform additional fine-tuning to ensure that the embedding distances are spatially or semantically grounded. This would involve collecting labeled data with grounded quantitative information about how similar or different two embeddings are, such as from known physical distances, or human intuition.

Another challenge is to *explain* the result of an ETL-based analysis (e.g., monitoring or falsification) in terms of concepts that are human understandable, rather than in the embedding space. One

direction that we plan to explore is to *decode* embeddings of interest (e.g., a violating trace) into the observation space (e.g., images) using a world model, similar to how it is done in [Zhou et al. \(2025\)](#); [Nakamura et al. \(2025\)](#). This would allow us to, for example, present the user with an explanation of a violation as a sequence of images, improving the interpretability of system behavior.

References

- Derya Aksaray, Austin Jones, Zhaodan Kong, Mac Schwager, and Calin Belta. Q-learning for robust satisfaction of signal temporal logic specifications, 2016.
- Jasmine Jerry Aloor, Jay Patrikar, Parv Kapoor, Jean Oh, and Sebastian Scherer. Follow the rules: Online signal temporal logic tree search for guided imitation learning in stochastic domains. In *2023 IEEE International Conference on Robotics and Automation (ICRA)*, pages 1320–1326, 2023. doi: 10.1109/ICRA48891.2023.10160953.
- Rajeev Alur, Osbert Bastani, Kishor Jothimurugan, Mateo Perez, Fabio Somenzi, and Ashutosh Trivedi. Policy synthesis and reinforcement learning for discounted ltl. In *International Conference on Computer Aided Verification*, pages 415–435. Springer, 2023.
- Anand Balakrishnan, Jyotirmoy Deshmukh, Bardh Hoxha, Tomoya Yamaguchi, and Georgios Fainekos. Percemon: online monitoring for perception systems. In *Runtime Verification: 21st International Conference, RV 2021, Virtual Event, October 11–14, 2021, Proceedings 21*, pages 297–308. Springer, 2021.
- Ezio Bartocci, Jyotirmoy Deshmukh, Alexandre Donzé, Georgios Fainekos, Oded Maler, Dejan Ničković, and Sriram Sankaranarayanan. Specification-Based Monitoring of Cyber-Physical Systems: A Survey on Theory, Tools and Applications. In Ezio Bartocci and Yliès Falcone, editors, *Lectures on Runtime Verification: Introductory and Advanced Topics*, Lecture Notes in Computer Science, pages 135–175. Springer International Publishing, Cham, 2018. ISBN 978-3-319-75632-5. doi: 10.1007/978-3-319-75632-5_5.
- Calin Belta and Sadra Sadraddini. Formal methods for control synthesis: An optimization perspective. *Annual Review of Control, Robotics, and Autonomous Systems*, 2(1):115–140, 2019. doi: 10.1146/annurev-control-053018-023717. URL <https://doi.org/10.1146/annurev-control-053018-023717>.
- Luca Bortolussi and Laura Nenzi. Specifying and monitoring properties of stochastic spatio-temporal systems in signal temporal logic. In *Proceedings of the 8th International Conference on Performance Evaluation Methodologies and Tools*, pages 66–73, 2014.
- Angel Chang, Angela Dai, Thomas Funkhouser, Maciej Halber, Matthias Niessner, Manolis Savva, Shuran Song, Andy Zeng, and Yinda Zhang. Matterport3d: Learning from rgb-d data in indoor environments. *International Conference on 3D Vision (3DV)*, 2017.
- Matthew Chang, Theophile Gervet, Mukul Khanna, Sriram Yenamandra, Dhruv Shah, So Yeon Min, Kavitha Shah, Chris Paxton, Saurabh Gupta, Dhruv Batra, Roozbeh Mottaghi, Jitendra Malik, and Devendra Singh Chaplot. Goat: Go to any thing, 2023. URL <https://arxiv.org/abs/2311.06430>.

- Mehdi Cherti, Romain Beaumont, Ross Wightman, Mitchell Wortsman, Gabriel Ilharco, Cade Gordon, Christoph Schuhmann, Ludwig Schmidt, and Jenia Jitsev. Reproducible scaling laws for contrastive language-image learning. In *Proceedings of the IEEE/CVF Conference on Computer Vision and Pattern Recognition*, pages 2818–2829, 2023.
- Adel Dokhanchi, Heni Ben Amor, Jyotirmoy V Deshmukh, and Georgios Fainekos. Evaluating perception systems for autonomous vehicles using quality temporal logic. In *Runtime Verification: 18th International Conference, RV 2018, Limassol, Cyprus, November 10–13, 2018, Proceedings 18*, pages 409–416. Springer, 2018.
- Alexey Dosovitskiy, Lucas Beyer, Alexander Kolesnikov, Dirk Weissenborn, Xiaohua Zhai, Thomas Unterthiner, Mostafa Dehghani, Matthias Minderer, Georg Heigold, Sylvain Gelly, Jakob Uszkoreit, and Neil Houlsby. An image is worth 16x16 words: Transformers for image recognition at scale, 2021. URL <https://arxiv.org/abs/2010.11929>.
- Georgios E. Fainekos and George J. Pappas. Robustness of temporal logic specifications for continuous-time signals. *Theor. Comput. Sci.*, 410(42):4262–4291, 2009.
- Roya Firoozi, Johnathan Tucker, Stephen Tian, Anirudha Majumdar, Jiankai Sun, Weiyu Liu, Yuke Zhu, Shuran Song, Ashish Kapoor, Karol Hausman, Brian Ichter, Danny Driess, Jiajun Wu, Cewu Lu, and Mac Schwager. Foundation models in robotics: Applications, challenges, and the future, 2023. URL <https://arxiv.org/abs/2312.07843>.
- David Ha and Jürgen Schmidhuber. World models. *CoRR*, abs/1803.10122, 2018. URL <http://arxiv.org/abs/1803.10122>.
- Iman Haghighi, Austin Jones, Zhaodan Kong, Ezio Bartocci, Radu Gros, and Calin Belta. Spatel: a novel spatial-temporal logic and its applications to networked systems. In *Proceedings of the 18th International Conference on Hybrid Systems: Computation and Control*, pages 189–198, 2015.
- Mohammad Hekmatnejad. *Formalizing safety, perception, and mission requirements for testing and planning in autonomous vehicles*. PhD thesis, Arizona State University, 2021.
- Mohammad Hekmatnejad, Bardh Hoxha, Jyotirmoy V. Deshmukh, Yezhou Yang, and Georgios Fainekos. Formalizing and evaluating requirements of perception systems for automated vehicles using spatio-temporal perception logic. *The International Journal of Robotics Research*, 43(2): 203–238, 2024. doi: 10.1177/02783649231223546. URL <https://doi.org/10.1177/02783649231223546>.
- Seth Hutchinson, Gregory D Hager, and Peter I Corke. A tutorial on visual servo control. *IEEE transactions on robotics and automation*, 12(5):651–670, 1996.
- Parv Kapoor, Kazuki Mizuta, Eunsuk Kang, and Karen Leung. Stlsg++: A masking approach for differentiable signal temporal logic specification. *arXiv preprint arXiv:2501.04194*, 2025.
- Ron Koymans. Specifying real-time properties with metric temporal logic. *Real-time systems*, 2(4): 255–299, 1990.

- Hadas Kress-Gazit, Georgios E Fainekos, and George J Pappas. Temporal-logic-based reactive mission and motion planning. *IEEE transactions on robotics*, 25(6):1370–1381, 2009.
- Alex Krizhevsky, Ilya Sutskever, and Geoffrey E Hinton. Imagenet classification with deep convolutional neural networks. In F. Pereira, C.J. Burges, L. Bottou, and K.Q. Weinberger, editors, *Advances in Neural Information Processing Systems*, volume 25. Curran Associates, Inc., 2012. URL https://proceedings.neurips.cc/paper_files/paper/2012/file/c399862d3b9d6b76c8436e924a68c45b-Paper.pdf.
- Karen Leung, Nikos Aréchiga, and Marco Pavone. Backpropagation through signal temporal logic specifications: Infusing logical structure into gradient-based methods. *The International Journal of Robotics Research*, page 02783649221082115, 2023.
- Lars Lindemann and Dimos V. Dimarogonas. Control barrier functions for signal temporal logic tasks. *IEEE Control Systems Letters*, 3:96–101, 2019. URL <https://api.semanticscholar.org/CorpusID:50767137>.
- Oded Maler and D. Nickovic. Monitoring temporal properties of continuous signals. In *FORMATS/FTRTFT*, 2004. URL <https://api.semanticscholar.org/CorpusID:15642684>.
- Claudio Menghi, Christos Tsigkanos, Patrizio Pelliccione, Carlo Ghezzi, and Thorsten Berger. Specification patterns for robotic missions. *CoRR*, abs/1901.02077, 2019. URL <http://arxiv.org/abs/1901.02077>.
- Kensuke Nakamura, Lasse Peters, and Andrea Bajcsy. Generalizing safety beyond collision-avoidance via latent-space reachability analysis, 2025. URL <https://arxiv.org/abs/2502.00935>.
- Maxime Oquab, Timothée Darcet, Théo Moutakanni, Huy Vo, Marc Szafraniec, Vasil Khalidov, Pierre Fernandez, Daniel Haziza, Francisco Massa, Alaaeldin El-Nouby, Mahmoud Assran, Nicolas Ballas, Wojciech Galuba, Russell Howes, Po-Yao Huang, Shang-Wen Li, Ishan Misra, Michael Rabbat, Vasu Sharma, Gabriel Synnaeve, Hu Xu, Hervé Jegou, Julien Mairal, Patrick Labatut, Armand Joulin, and Piotr Bojanowski. Dinov2: Learning robust visual features without supervision, 2024. URL <https://arxiv.org/abs/2304.07193>.
- Amir Pnueli. The temporal logic of programs. In *18th Annual Symposium on Foundations of Computer Science*, pages 46–57. IEEE Computer Society, 1977.
- Alec Radford, Jong Wook Kim, Chris Hallacy, Aditya Ramesh, Gabriel Goh, Sandhini Agarwal, Girish Sastry, Amanda Askell, Pamela Mishkin, Jack Clark, Gretchen Krueger, and Ilya Sutskever. Learning transferable visual models from natural language supervision, 2021a. URL <https://arxiv.org/abs/2103.00020>.
- Alec Radford, Jong Wook Kim, Chris Hallacy, Aditya Ramesh, Gabriel Goh, Sandhini Agarwal, Girish Sastry, Amanda Askell, Pamela Mishkin, Jack Clark, et al. Learning transferable visual models from natural language supervision. In *International conference on machine learning*, pages 8748–8763. PMLR, 2021b.

- Vasumathi Raman, Alexandre Donze, Mehdi Maasoumy, Richard M Murray, Alberto Sangiovanni-Vincentelli, and Sanjit Seshia. Model predictive control with signal temporal logic specifications. In *Conference on Decision and Control*, 2014.
- Manolis Savva, Abhishek Kadian, Oleksandr Maksymets, Yili Zhao, Erik Wijmans, Bhavana Jain, Julian Straub, Jia Liu, Vladlen Koltun, Jitendra Malik, Devi Parikh, and Dhruv Batra. Habitat: A Platform for Embodied AI Research. In *Proceedings of the IEEE/CVF International Conference on Computer Vision (ICCV)*, 2019.
- Sanjit A. Seshia, Ankush Desai, Tommaso Dreossi, Daniel J. Fremont, Shromona Ghosh, Edward Kim, Sumukh Shivakumar, Marcell Vazquez-Chanlatte, and Xiangyu Yue. Formal specification for deep neural networks. In *Automated Technology for Verification and Analysis*, pages 20–34, 2018.
- Dawei Sun, Jingkai Chen, Sayan Mitra, and Chuchu Fan. Multi-agent motion planning from signal temporal logic specifications. *IEEE Robotics and Automation Letters*, PP:1–1, 2022. URL <https://api.semanticscholar.org/CorpusID:245986629>.
- Manuel Watter, Jost Tobias Springenberg, Joschka Boedecker, and Martin Riedmiller. Embed to control: A locally linear latent dynamics model for control from raw images, 2015. URL <https://arxiv.org/abs/1506.07365>.
- Gaoyue Zhou, Hengkai Pan, Yann LeCun, and Lerrel Pinto. Dino-wm: World models on pre-trained visual features enable zero-shot planning, 2025. URL <https://arxiv.org/abs/2411.04983>.

Appendix A. Distance Metrics over Image Embeddings

We provide descriptions of the four distance metrics that we have investigated for ETL so far:

- **L1 norm.** L1 norm or manhattan distance computes the absolute differences between the corresponding elements in two embedding vectors. It is defined as: $d_{L1}(A, B) = \sum_i |a_i - b_i|$, where $A = \{a_i\}$ and $B = \{b_i\}$ represent embedding vectors. The L1 norm is a robust metric that is particularly useful in scenarios where outliers need to be ignored.
- **L2 norm.** L2 norm is one of the most commonly used distance metrics for embeddings. It computes the straight-line distance between two vectors and is defined as: $d_{L2}(A, B) = \sqrt{\sum_i (a_i - b_i)^2}$. The L2 norm effectively captures granular differences between dense embeddings and is sensitive to large variations in feature values.
- **Chamfer Distance** Chamfer Distance (CD) is a metric used to compare two sets of points by computing the sum of minimized distances between them. Given two sets of patch embeddings, $A = \{a_i\}_{i=1}^N$ and $B = \{b_j\}_{j=1}^M$, the Chamfer Distance is defined as: $d_C(A, B) = \sum_{a \in A} \min_{b \in B} \|a - b\|_2^2 + \sum_{b \in B} \min_{a \in A} \|a - b\|_2^2$. This metric ensures that every patch embedding in one set is matched to the closest embedding in the other set, capturing structural similarity between the two distributions. Unlike global feature-based similarity measures, it preserves local correspondences and is hence useful for comparing high-dimensional representations such as DINOv2 patch embeddings. Note that chamfer distance is a quasi-metric as it does not satisfy the triangle inequality.
- **Cosine Similarity** Cosine similarity measures the cosine of the angle between two embedding vectors and captures high level directional similarity. It is defined as:

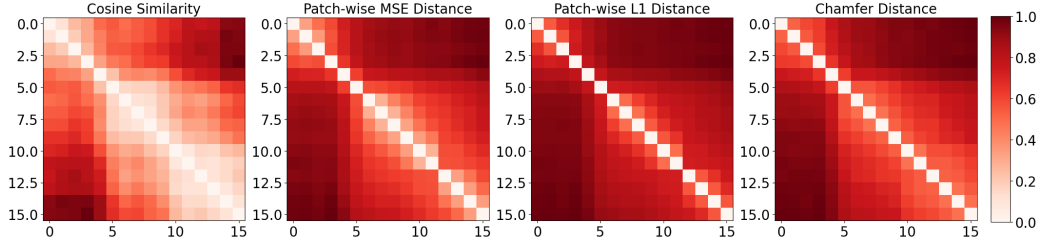
$$\text{cosine similarity}(A, B) = \frac{A \cdot B}{\|A\|_2 \|B\|_2}$$

where A and B are embedding vectors, $A \cdot B$ is their dot product, and $\|A\|_2$ and $\|B\|_2$ are the L2 norms of the vectors. Cosine similarity ranges from -1 (completely dissimilar) to 1 (completely aligned). A value of 0 indicates the orthogonality of the two vectors. It is particularly useful for comparing the orientation of embeddings and has been successfully used to compare image similarity when used for content-based image retrieval.

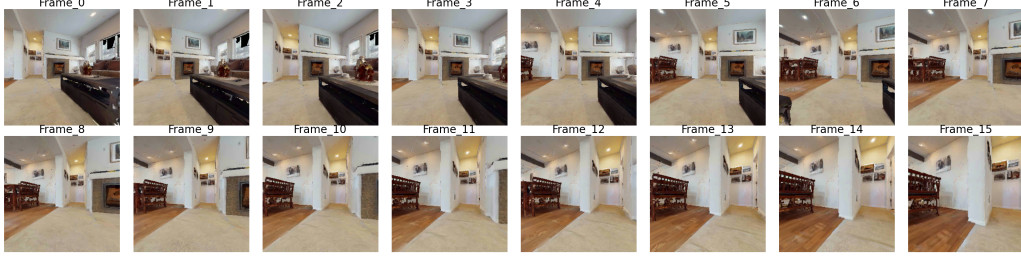
The distance comparison between a larger set of images is provided in the Figure 3.

Appendix B. Textual and Image Embeddings

In this section, we talk about distance metrics between multimodal embeddings, specifically text embeddings and image embeddings. In order for a meaningful comparison between these embeddings, they both need to exist in the same latent space. Pre-trained models such as the CLIP model (Contrastive Language Image Pretraining) are trained jointly on images and texts for image captioning tasks [Radford et al. \(2021b\)](#). Due to this joint pretraining, there have been multiple works that leverage CLIP’s pre-trained text and image encoders for other applications due to their rich feature representation. Inspired by CLIP’s original training objective that uses cosine similarities between text and image embeddings, we also define our distance metric between multimodal embeddings



(a) Embedding distance metric computation for Dino features



(b) Ground truth images used for distance computation

Figure 3: Image-to-image embedding distances We compute distance metrics between the embeddings of images captured within a Habitat scene. Each image is processed by a pretrained encoder, from which we extract the corresponding embeddings. We then calculate the pairwise distances between these embeddings using different distance metrics.

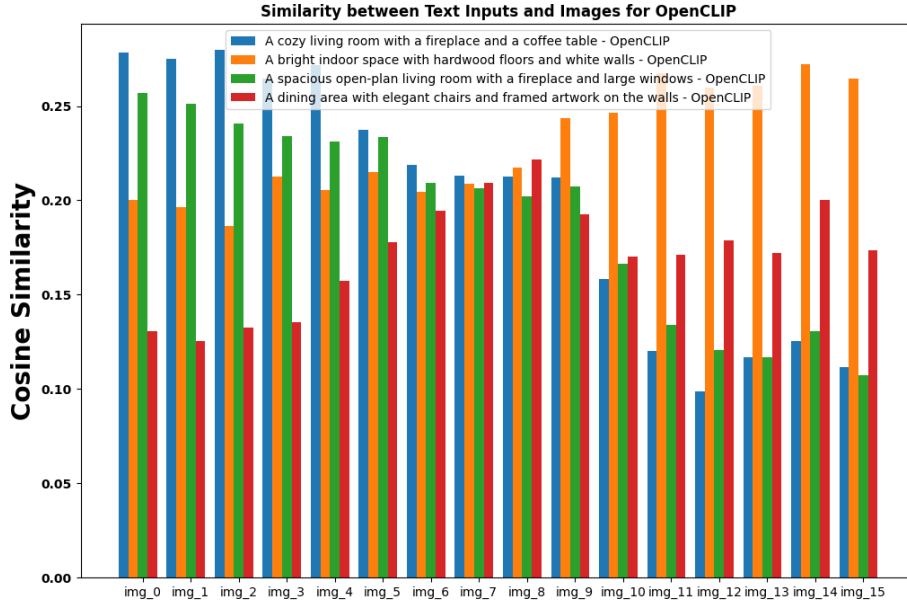


Figure 4: Text-image embedding distances We demonstrate how models like OpenCLIP can generate textual embeddings that can be compared with image embeddings. This enables the capture of arbitrary requirements through text while serving as a reliable specification mechanism for behavior.



Figure 5: Ending states after planning with a pretrained PACT world model in Habitat environment using L2 distance as the base metric. We present the start state as well as the goal images used for φ_1 , φ_2 , and φ_3 in different scenes. The planner is able to successfully achieve positive satisfaction scores for all ETL specifications.

using cosine similarity scores. Note that cosine similarity does not satisfy the triangle inequality so it is not a metric over the embedding space in the conventional sense but we plan to investigate other metrics that satisfy this property in future work.

We highlight our computed cosine similarity scores between different textual prompt embeddings and image embeddings in Figure 4. The images processed by the pretrained model are shown in Figure 3. We compute the text and image embeddings using OpenCLIP Cherti et al. (2023) model which is a state of the art model for image captioning. We observe that the cosine similarity scores for the prompt with “fireplace and coffee table” is higher for images 0–7 and goes down progressively as these objects are not visible in the scene for images 8–15. Conversely, We observe increasing similarity scores for the prompt with “hardwood floors and white walls” as these objects are visible in the images 8–15 and not in the previous frames. This shows that user provided textual prompts can be used directly to guide behavior generation via computing distances with image embeddings. By simply comparing prompts with scene images, an agent can prioritize actions or viewpoints that match the user’s goals the most.

Appendix C. Navigation with ETL Specifications

We provide some qualitative results of planning with a PACT world model to satisfy ETL specifications. with L2 as the base distance metric. We picked various scenes in the habitat environment and passed target images from those environments. The start, goal and final states are highlighted in Figure 5. The planner is able to achieve complex behaviors like sequential visits and either-or for a variety of environments.

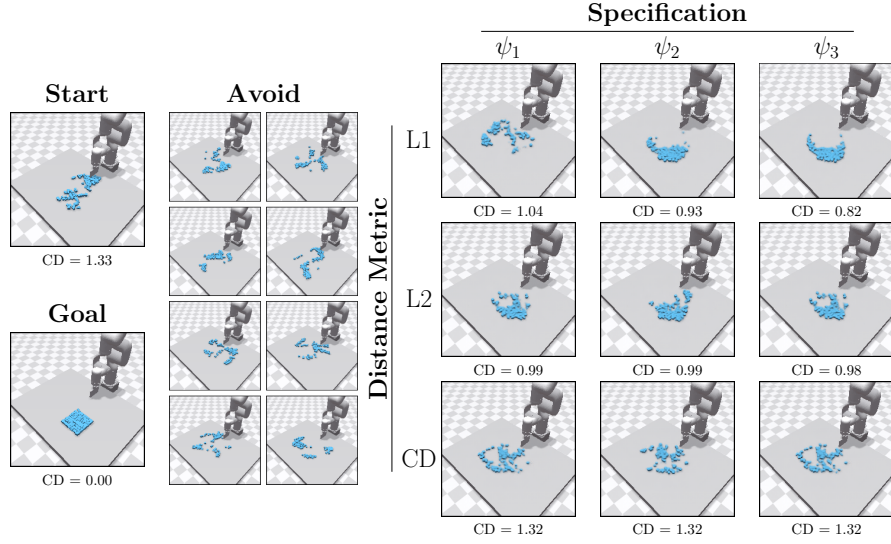


Figure 6: Ending configurations of granules after planning with a horizon length 10 with the Dino World Model. We present the initial configuration as well as the target specification for ψ_1 and ψ_3 , and images used for avoidance in ψ_2 and ψ_3 . Planning was done over embedded images with L1 norm, L2 norm, and chamfer distances, with the final chamfer distance for success evaluation shown was computed against the ground truth target.

Appendix D. Manipulation with ETL Specifications

We present the images used for ETL specifications in Figure 6. We can observe that computing chamfer distances over the embedded images does not greatly reduce the ending chamfer distance from the starting goal in the observed space, while using L1 norm and L2 norm for the distance metrics is more effective to manipulating the granules to the target specification. Additionally, we note that there are strong similarities between the ending configurations for L2 ψ_1 and L2 ψ_3 , as well as CD ψ_1 and CD ψ_3 , while L1 ψ_2 and L1 ψ_3 share stronger similarities. ETL specifications here have assisted with avoid and avoid-reach planning for manipulation. L1 ψ_2 specifically shows that even without a target goal to reach, ETL specifications assist with planning towards an unknown target. With optimization of planning for ETL specific specifications, manipulation planning can be improved from only planning with a single reach target.